Journal of Alloys and Compounds 655 (2016) 60–65

Contents lists available at ScienceDirect

Journal of Alloys and Compounds

journal homepage: http://www.elsevier.com/locate/jalcom

Characterization and microwave dielectric properties of wolframite-type $MgZrNb_2O_8$ ceramics

J.D. Guo, J.X. Bi, Q.J. Mei, H.T. Wu*

Shandong Provincial Key Laboratory of Preparation and Measurement of Building Materials, University of Jinan, Jinan, 250022, China

ARTICLE INFO

Article history:
Received 6 August 2015
Received in revised form
12 September 2015
Accepted 15 September 2015
Available online 25 September 2015

Keywords:
$MgZrNb_2O_8$
Sol-gel process
Solid-state method
Microwave dielectric properties

ABSTRACT

Wolframite type $MgZrNb_2O_8$ ceramics were prepared by solid-state method and sol–gel process in this study, and the influence of sol–gel process on the sintering behavior and microwave dielectric properties of $MgZrNb_2O_8$ ceramics was investigated. The optimal sintering temperatures of $MgZrNb_2O_8$ ceramic for solid-state and sol–gel method were 1225 °C and 1175 °C, respectively. For solid-state method, MZN ceramics sintered at 1225 °C with nearly full density had the microwave dielectric properties of $\varepsilon_r = 27.08$, $Q{\cdot}f = 29{,}070$ GHz and $\tau_f = -24.31$ ppm/°C. For sol–gel process, MZN ceramics sintered at 1175 °C with nearly full density had excellent microwave dielectric properties of $\varepsilon_r = 22.16$, $Q{\cdot}f = 29{,}490$ GHz and $\tau_f = -15.99$ ppm/°C. Obviously, sol–gel synthetic route could significantly reduce the sintering temperature and improve the microwave dielectric properties.

1. Introduction

In recent decades, microwave dielectric ceramics developed rapidly, and have been the basis for the realization of microwave control function and the key materials to the microwave devices (such as resonator, phase shifter, etc.) widely used in modern communication [1–4]. In order to meet the demand for miniaturization and integration, it is increasingly needed to expand the search for new microwave dielectric materials, which should have appropriate dielectric constant (ε_r), high quality factor ($Q{\cdot}f$), near-zero temperature coefficient of resonant frequency (τ_f) [5]. At present, many types of compounds were reported for the possible use in microwave applications [6–10]. Among several kinds of microwave dielectric ceramics with low dielectric constant, wolframite-type $MgZrNb_2O_8$ (MZN) ceramics possess excellent properties, high quality factors combined with appropriate dielectric constant.

MZN ceramics were always prepared by the conventional solid-state method in the past reports [11,12]. For instance, Y. Cheng et al. [11] reported that MZN ceramic was obtained at 1340 °C for 4 h by the solid-state method with $\varepsilon_r = 26$, $Q{\cdot}f = 120{,}816$ GHz and $\tau_f = -50.2$ ppm/°C. In addition, S.D. Ramarao and V.R.K. Murthy [12] also reported that the MZN ceramics could be sintered at 1500 °C via the traditional solid-state method and exhibited the microwave dielectric properties: $\varepsilon_r = 9.60$, $Q{\cdot}f = 58{,}500$ GHz and $\tau_f = -31.5$ ppm/°C. As reported in the past, the major disadvantage of solid-state method was higher sintering temperature. Sol–gel process not only had advantages of high purity and homogeneous grain size, but also lowered the sintering temperature as well as improved the dielectric properties. However, little research regarding preparation of MZN ceramics by the aqueous sol–gel process has been reported in the literature to date. In the following study, a wolframite MZN ceramic was prepared by solid-state method and sol–gel process. The effects of sol–gel process on sintering temperature, phase compositions, microstructures and microwave dielectric properties of MZN ceramics were also investigated in detail.

2. Experimental procedure

High-purity oxide MgO (99%), ZrO_2 (99.99%) and Nb_2O_5 (99.9%) were used as raw materials to synthesize the MZN powders by the solid state method. The raw materials were weighed and mixed according to the formula of $MgZrNb_2O_8$. The mixed powders were ball-milled for 8 h with distilled water in a nylon container with ZrO_2 balls. All the slurries were dried and pre-sintered at 1050 °C for 4 h to obtain single phase MZN. Then the powders were re-milled for 6 h. Analytical-grade $Mg(NO_3)_2{\cdot}6H_2O$, $Zr(NO_3)_4{\cdot}5H_2O$, Nb_2O_5, citric acid (CA) and ethylene glycol (EG) were used as raw materials to synthesize the MZN nanopowders by the sol–gel

* Corresponding author.
E-mail address: mse_wuht@ujn.edu.cn (H.T. Wu).

http://dx.doi.org/10.1016/j.jallcom.2015.09.143
0925-8388/

method. Firstly, a stoichiometric amount of Nb_2O_5 was dissolved in hydrofluoric acid to get its ionic solution. Secondly, aqueous ammonia was added slowly to the previous solution to obtain precipitate. Thirdly, the precipitate was filtered and washed with deionized water several times to remove F^- ions and then dissolved completely in citric acid aqueous solution by continuous magnetic stirring at 300 rpm for 15 min. The whole formation process could be formulated from Eqs. (1)–(2). Meanwhile, a stoichiometric amount of $Mg(NO_3)\cdot 6H_2O$ and $Zr(NO_3)_4\cdot 5H_2O$ were added to the mixing citric solution of Nb to get the Mg–Zr–Nb solution. Finally, ethylene was added to the mixed solution and stirred for 1 h to form a transparent and stable sol. pH of the solution was controlled around 4 by adding buffering agents. The resulting sol was left evaporating at 80°C–90 °C until a viscous gel-like product was formed and then subsequently calcined by a slow heating in air atmosphere from 600°C to 900 °C. The calcined powders were remilled in a polyethylene jar for 6 h using ZrO_2 balls to reduce conglobation. The dried powders synthesized by solid-state and sol–gel method were mixed with high purity paraffin as a binder at 60 °C, granulated and pressed into cylindrical disks of 10 mm in diameter and about 5 mm in thickness at a pressure of about 200 MPa. These pellets were preheated at 500 °C for 4 h to expel the binder and then sintered at 1100 °C −1275 °C for 4 h in air at a heating rate of 5 °C/min.

$$Nb_2O_5 + 10HF \rightarrow 2NbOF_5^{2-} + 4H^+ + 3H_2O \quad (1)$$

$$NbOF_5^{2-} + 5NH_3\cdot H_2O + H_2O \rightarrow 5NH_4^+ + Nb(OH)_5\downarrow + 2OH^- + 5F^- \quad (2)$$

Phase analysis of samples was conducted with the help of a Rigaku diffractometer (Model D/MAX-B, Rigaku Co., Japan) using Ni filtered CuKα radiation (λ = 0.1542 nm) at 40 kV and 40 mA settings. Based on XRD analysis, the morphology and particle sizes were examined using a transmission electron microscopy (Model JEOL JEM-2010, FEI Co., Japan) coupled with energy dispersive X-ray spectroscopy (EDS). A network analyzer (N5234A, Agilent Co., America) was used for the measurement of microwave dielectric properties. Dielectric constants were measured using Hakki–Coleman post-resonator method by exciting the TE011 resonant mode of dielectric resonator by using an electric probe as suggested by Hakki and Coleman [13]. Unloaded quality factors were measured using TE01d mode by the cavity method [14]. All measurements were made at room temperature and in the frequency of 8–12 GHz. Temperature coefficients of resonant frequency were measured in the temperature range of 25°C–85 °C. The apparent densities of the sintered pellets were measured use the Archimedes method (Mettler ToledoXS64).

3. Results and discussion

The X-ray diffraction patterns of MZN powders calcined at 900°C–1100 °C for 2 h are illustrated in Fig. 1(a). As shown in Fig. 1(a), ZrO_2 (JCPDS No. 83-0938) as secondary phase was observed at 900 °C, and the peak intensity of it decreased with the calcining temperature increasing. It is obvious that powders were not reacted completely at lower temperature. There was no significant change in the X-ray diffraction patterns of MZN powders with the calcining temperature increasing from 1000 °C to 1100 °C. However, it was pleasantly found that the crystallization of wolframite-structure MZN as predominant phase took place at 1050 °C, which was in agreement with the XRD pattern of JCPDS No. 48-0329. The XRD patterns of MZN xerogel calcined at temperatures ranging from 600 °C to 900 °C for 60 min in air atmosphere are shown in Fig. 1(b). Similarly, there was no significant change for the diffraction patterns in the range of 600°C–900 °C, and it can be found that the crystallization of MZN as predominant phase took place at 600 °C in view of diffraction peaks from significant lattice planes, such as (111), (−110), and (130). The XRD patterns of the xerogel fired at 800 °C and 900 °C still consisted of predominant peaks of ZTN with sharper peaks free from any secondary phases. Therefore, according to XRD result it was indicated that calcinations temperature of synthesizing wolframite-type MZN phase was remarkably decreased to 600 °C by the sol–gel process, which was lower than the conventional mixed oxide route.

Fig. 2 shows the shrinking ratio and apparent density of MZN samples as a function of sintering temperatures, and the optimal sintering temperature can be got through this figure. The shrinkage variations of the samples were characterized by the ratio of the diametric size, and the theoretical density of MZN ceramic was 5.18 g/cm^3 obtained from the crystal structure and atomic weight [15]. As shown in Fig. 2(a), the shrinking ratio of samples prepared by sol–gel process increased from 16.91% to 18.77% with the sintering temperature increasing in the region of 1100°C–1200 °C. And the apparent density increased from 4.32 g/cm^3 to 4.86 g/cm^3 with the sintering temperature increasing from 1100 °C to 1175 °C, which was due to the decrease of pores and the improvement of grains as sintering temperature increased shown in Fig. 5(a)–(c). At 1175 °C, a maximum value of apparent densities reached 4.86 g/cm^3. However, when the sintering temperature was over 1175 °C the density decreased sharply, which was due to abnormal grain growth observed in the samples.

Based on the results of sintering characteristics, it was found that the MZN ceramic prepared by sol–gel process with nearly full density was obtained at the 1175 °C for 4 h. The variation of shrinking ratio and apparent density of MZN samples prepared by solid-state method was shown in Fig. 2(b). As shown in Fig. 2(b), it could be easily found that the apparent density increased rapidly in the temperature region of 1100°C–1225 °C, a saturated value of apparent density was found to be nearly 4.87 g/cm^3 at 1225 °C and the curve of diametric shrinkage ratio also showed a similar tendency. So the optimal sintering temperature of MZN ceramic prepared by solid-state method can be obtained at 1225 °C for 4 h. By comparison, it was concluded that MZN ceramics could be obtained at lower sintering temperatures by the aqueous sol–gel process, which was due to the fact that the specific surface energy and driving force for sintering were increased by the decreasing particle size and refining microstructure in sol–gel route.

The X-ray diffraction patterns of MZN ceramics sintered at different temperatures were illustrated in Fig. 3. It was found that all the samples exhibited $MgZrNb_2O_8$ with the space group of P2/c as a main crystalline phase, which was in agreement with the XRD pattern of JCPDS No. 48–0329. And the X-ray diffraction patterns of MZN ceramics by solid-state and sol–gel method were not changed significantly in the whole temperature range, respectively. Moreover, a small amount of secondary phase was observed. For sol–gel process, the secondary phase of $MgNb_2O_6$ was observed at 48°–49° in the whole range. And for solid-state method, the secondary phase of $Mg_4Nb_2O_9$ was observed at 25°–26° in 1100 °C, and it was also observed at 53°–54° and 63°–64° in the whole temperature range. In addition, a small peak of Nb_2O_5 was existed at 28°–29° in 1100 °C, which was due to the incomplete reaction at lower sintering temperature.

SEM micrographs and EDS of samples prepared by solid-state method from 1100 °C to 1275 °C for 4 h are illustrated in Fig. 4. And the SEM micrographs and EDS for samples prepared by sol–gel process from 1100 °C to 1200 °C are shown in Fig. 5. In both cases, an increase in grain size and the decrease of pores were the

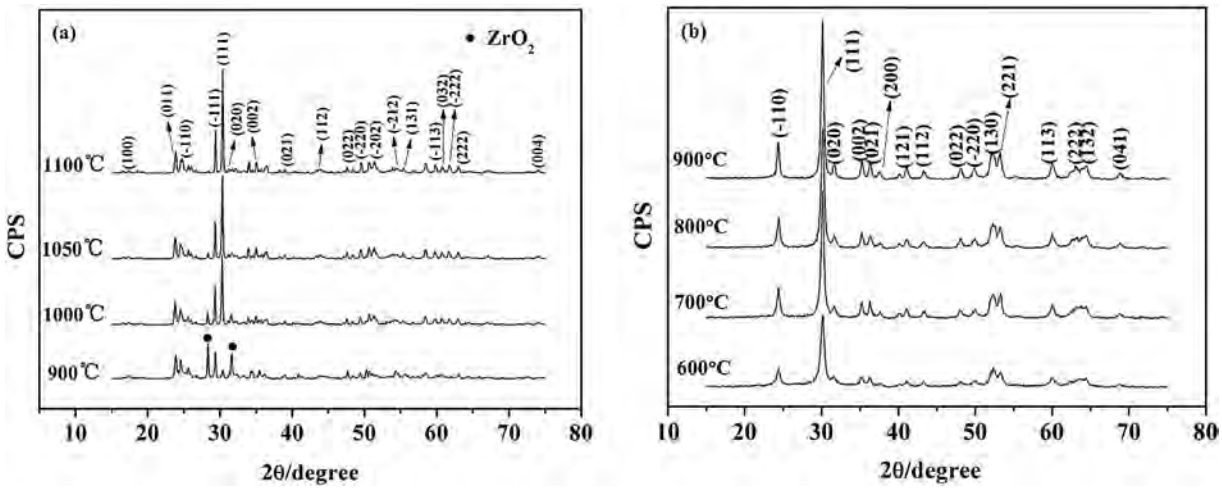

Fig. 1. XRD patterns of MZN powders at different temperature ((a) MZN powders pre-sintered at 900°C–1100 °C prepared by solid-state method; (b) Mg–Zr–Nb xerogel calcined at 600°C–900 °C prepared by sol–gel process).

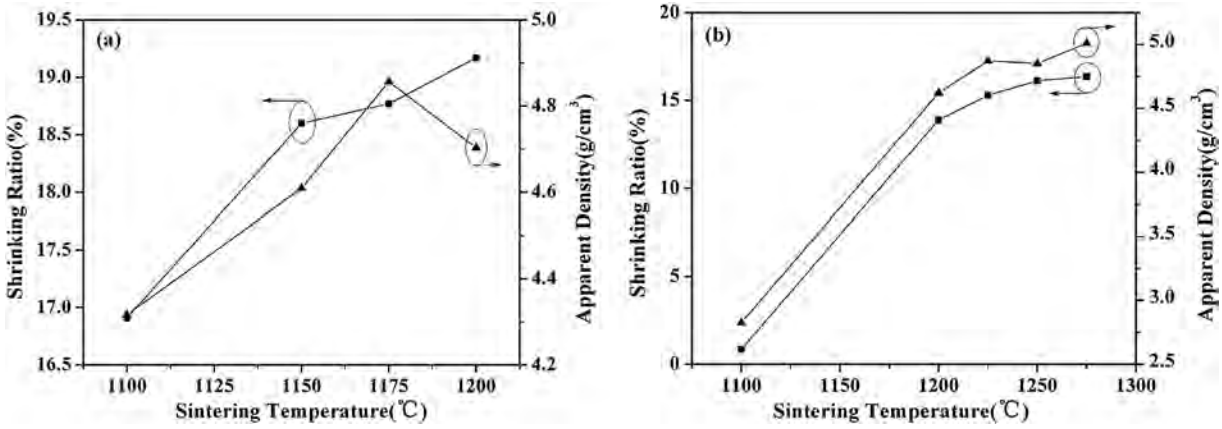

Fig. 2. Sintering behavior of $MgZrNb_2O_8$ ceramics as a function of sintering temperatures ((a) sol–gel process; (b) solid-state method).

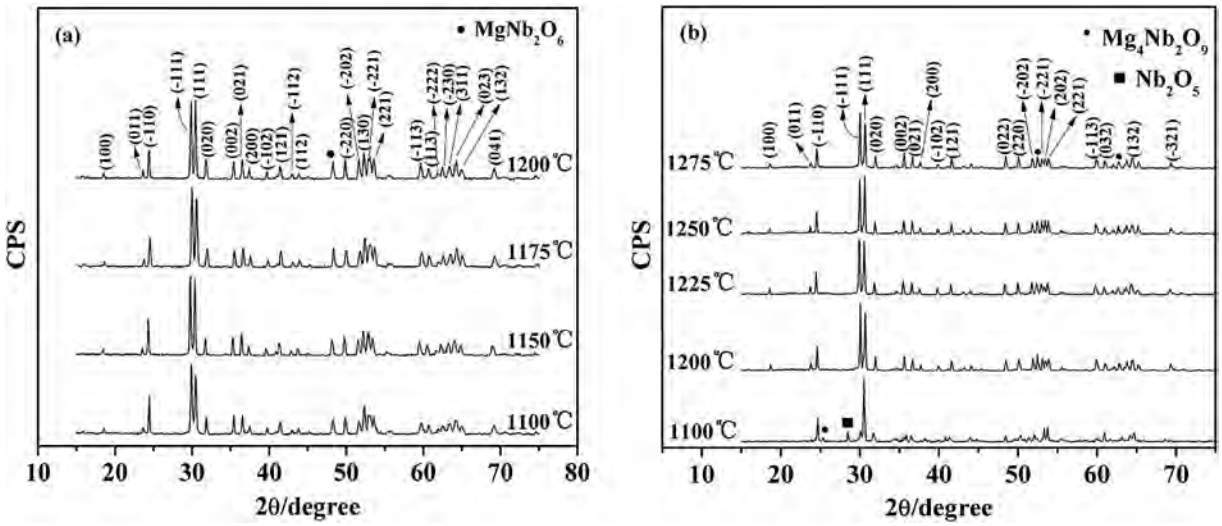

Fig. 3. XRD patterns of MZN ceramics sintered at different temperatures ((a) sol–gel process; (b) solid-state method).

common feature with the sintering temperature increasing, which was consistent with the results of the apparent density shown in Fig. 2. In Fig. 4, as sintering temperature increased to 1200 °C, porosity decreased rapidly and all pores almost disappeared at

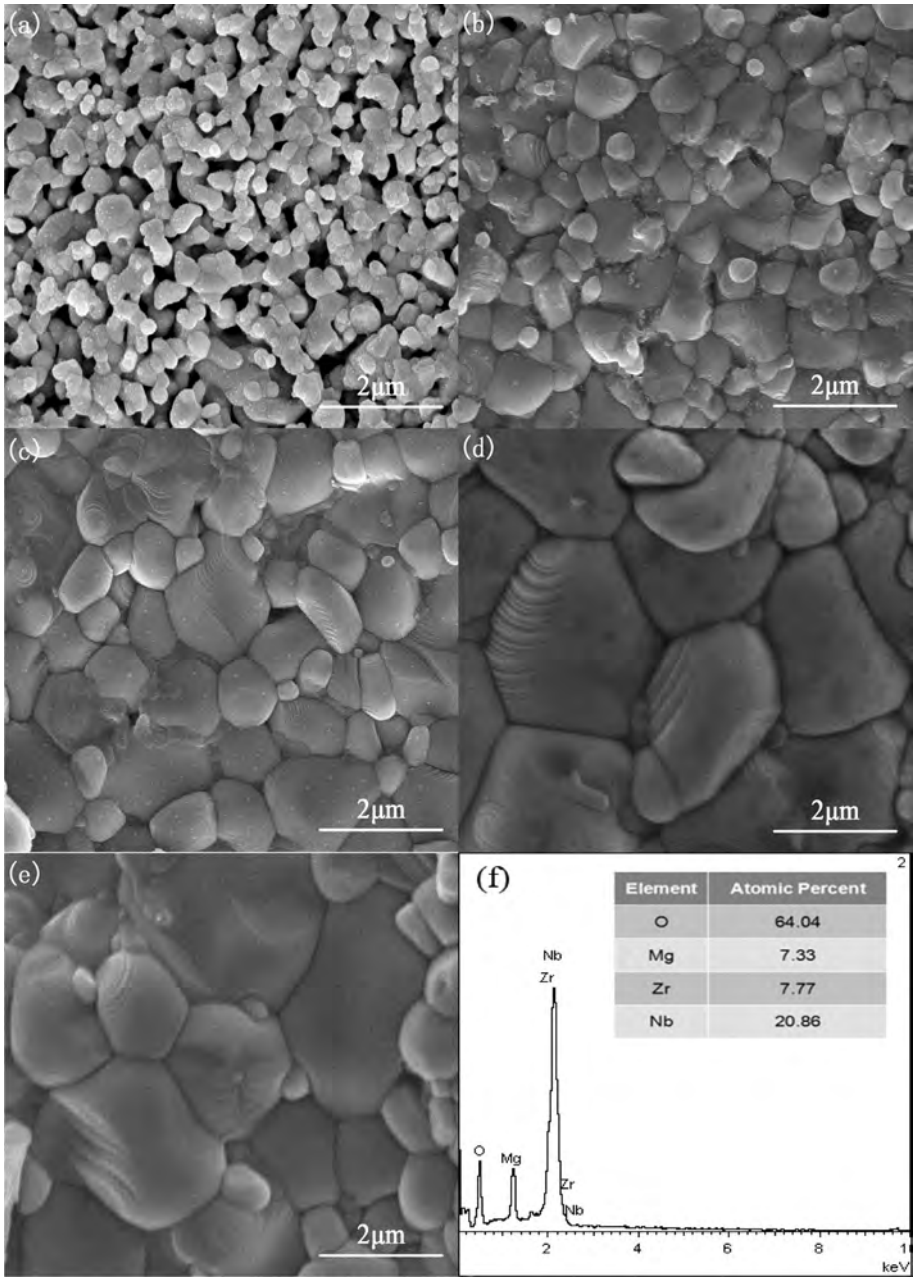

Fig. 4. SEM micrographs and EDS of MZN ceramics sintered at (a) 1100 °C, (b)1200 °C, (c) 1225 °C, (d) 1250 °C, (e) 1275 °C for 4 h by solid-state method and (f) EDS analysis.

1225 °C on the surface of MZN samples. The dense microstructure with low porosity and well-formed spheric-shape grains (1–2 μm) was obtained at 1225 °C shown in Fig. 4(c). However, when the sintering temperature was higher than 1225 °C, abnormal grain growth appeared shown in Fig. 4(d)–(e). Abnormal grain growth could be found as shown in Fig. 4(d)–(e) when sintering temperature was over 1225 °C. Similarly, MZN samples were prepared with full density through the sol–gel process at 1175 °C for 4 h, which was lower than that by solid-state reaction methods. And average grain sizes were measured approximately 50 nm at 1175 °C as shown in Fig. 5(c). By comparison, average grain size for sample prepared by sol–gel process was much smaller than that by the conventional method. In addition, EDS analysis about grains chosen randomly from the samples prepared by solid-state method and sol–gel process were also shown in Figs. 4 and 5, which presented a quantitative result about elementary composition. In both cases, the ratio of Mg/Zr/Nb/O was approximately corresponding to the formula of MZN phase.

Fig. 6 demonstrates the changes of ε_r, $Q{\cdot}f$ and τ_f values depending on sintering temperatures. As shown in Fig. 6(a), with the sintering temperature increasing from 1100 °C to 1200 °C, the ε_r values of MZN ceramics increased firstly in the temperature region of 1100°C–1150 °C, and then decreased when the sintering temperature was over 1150 °C. The increase at first was due to the densification of MZN ceramics, and the decrease in dielectric constant may be ascribed to the abnormal grain growth appearing at higher sintering temperature. And the value of ε_r in the optimal sintering temperature (1175 °C) is 22.16, which was lower than the dielectric constant (~27.08) of MZN ceramic prepared by solid-state method sintered at 1225 °C shown in Fig. 6(b).

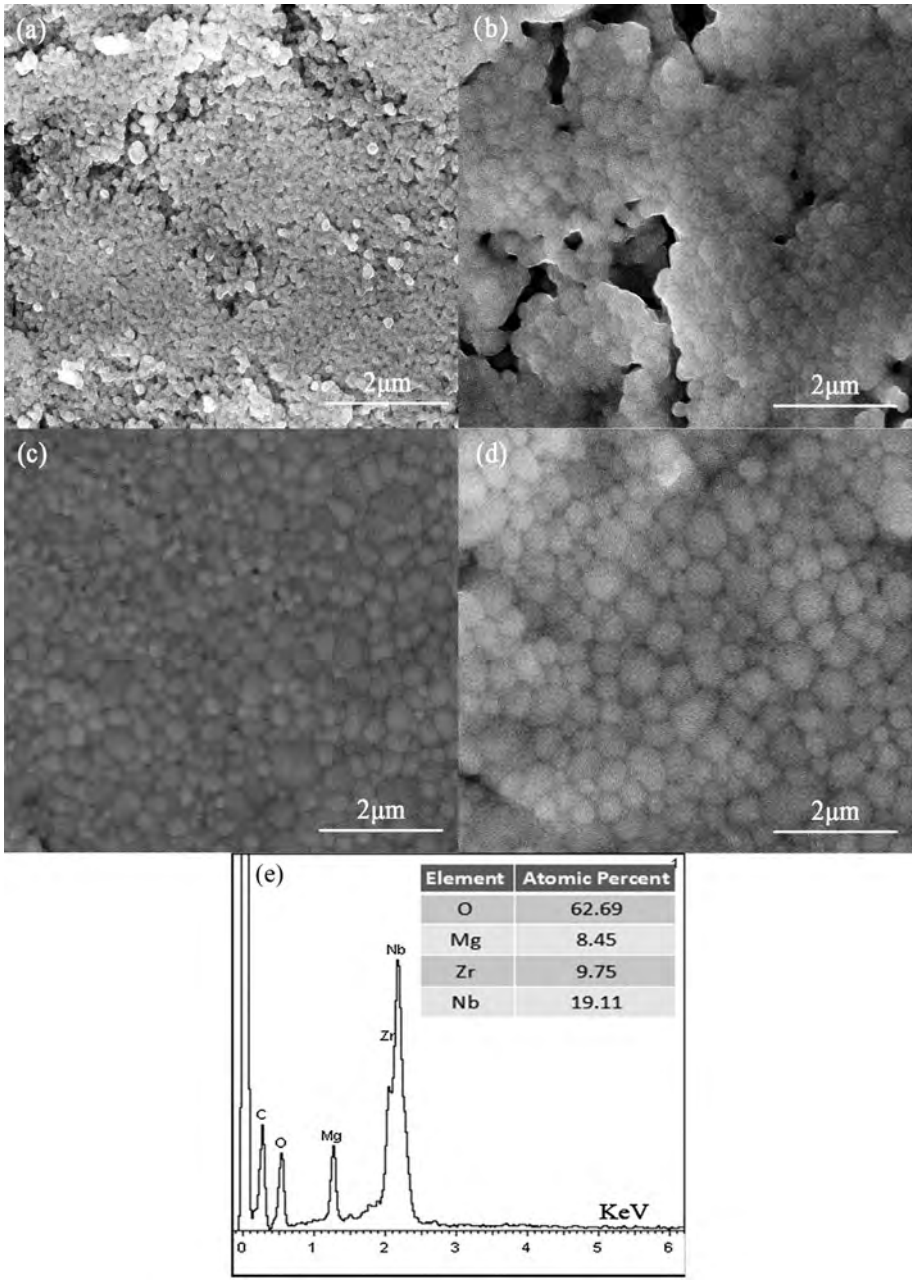

Fig. 5. SEM micrographs and EDS of MZN ceramics sintered at (a) 1100 °C, (b)1150 °C, (c) 1175 °C, (d) 1200 °C for 4 h by sol–gel process and (e) EDS analysis.

With the increase of sintering temperatures from 1100 °C to 1175 °C, $Q{\cdot}f$ values increased from 13,093 GHz to 29,486 GHz and then decreased to 28,500 GHz at 1200 °C, which was in accordance with the tendency of apparent density shown in Fig. 2. Therefore, the optimal $Q{\cdot}f$ value of 29,486 GHz was obtained when the MZN compounds was sintered at 1175 °C for 4 h. As we all know, the microwave dielectric loss includes not only intrinsic losses mainly caused by the lattice vibration modes but also extrinsic losses dominated by densification/porosity, the secondary phases, grain sizes and oxygen vacancies [16]. Among these factors, porosity was suggested to affect $Q{\cdot}f$ values obviously below 1175 °C. The remarkable increase in $Q{\cdot}f$ values in the range of 1100°C–1175 °C was associated with the decrease of porosity according to results of the sintering characteristic curves and SEM microstructure shown in Figs. 2 and 5(a–c), respectively. Some investigations [17,18] also reported that when the relative density was higher than 90%, the $Q{\cdot}f$ value was no longer dependent on density and porosity. That is to say, once the prepared samples reached nearly full density, $Q{\cdot}f$ values were mainly affected by intrinsic factors. So the decrease in $Q{\cdot}f$ values could be attributed to the non-uniform microstructure caused by abnormal grain growth shown in Fig. 5(d).

In addition, the presence of a small amount of secondary phase also had a certain influence on $Q{\cdot}f$ values. According to the results of the XRD patterns of MZN ceramics prepared by sol–gel process shown in Fig. 3(a), the secondary phase of $MgNb_2O_6$ whose microwave dielectric properties were $\varepsilon_r = 21.4$, $Q{\cdot}f = 93{,}800$ GHz and $\tau_f = -70$ ppm/°C sintered at 1300 °C [19] was observed in the whole temperature range. Compared to the $Q{\cdot}f$ value (~29,070 GHz) of MZN ceramic prepared by solid-state method sintered at 1225 °C shown in Fig. 6(b), the $Q{\cdot}f$ values of MZN ceramics could be

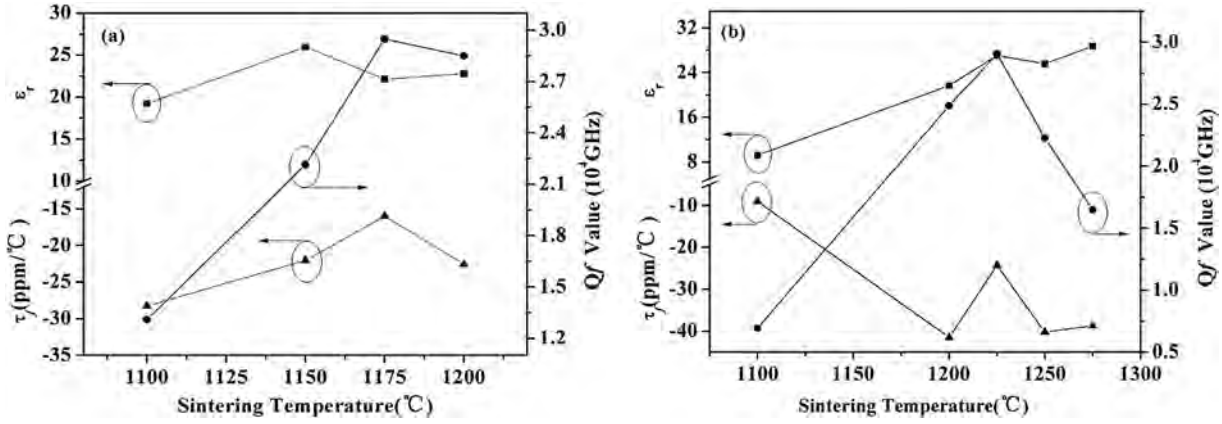

Fig. 6. Curves of ε_r, $Q{\cdot}f$ and τ_f values as a function of sintering temperatures for MZN ceramics ((a) sol–gel process; (b) solid-state method).

improved slightly by sol–gel process. According to Schlomann's theory, dielectric loss tangent at microwave frequency is mainly determined by the anharmonic terms in the crystal's potential energy [20,21]. Dielectric ceramics have many kinds of structural or lattice defects such as grain boundaries, voids, dislocations, point defects and substitutional ions. Rustum Roy reported that using the solution-sol-gel route had been developed to make a variety of ceramic materials, which provided major advantages in lowering sintering temperatures, refining microstructure, and controlling morphology and final phase composition [22]. The wolframite-structure MZN precursors were provided with well crystalline and less lattice defects for the fabrication of ceramics by the solution-sol-gel route in this work, which should contribute to the improvement of $Q{\cdot}f$ values.

Moreover, the temperature coefficient of resonant frequency (τ_f) was related to the composition, the additives and the secondary phase. The τ_f values of MZN ceramics prepared by sol–gel process increased to −15.99 ppm/°C firstly and then decreased in the region of 1100°C–1200 °C. However, τ_f values of MZN ceramics prepared by solid-state method fluctuated around −30 ppm/°C with sintering temperatures increasing from 1100 °C to 1275 °C and τ_f values were ranged from −9 ppm/°C to −41 ppm/°C. By comparison, the τ_f value was improved to −15.99 ppm/°C by sol–gel process. Hence, it was obvious that the improvement in the τ_f value was required for applications in electronics.

4. Conclusions

$MgZrNb_2O_8$ ceramics with wolframite type were prepared by solid-state method and sol–gel process in this study, and the influence of sol–gel process on sintering temperature, phase compositions, microstructures and microwave dielectric properties of MZN ceramics were also investigated. For solid-state method, MZN ceramics with nearly full densities were obtained at 1225 °C with microwave dielectric properties of $\varepsilon_r = 27.08$, $Q{\cdot}f = 29{,}070$ GHz and $\tau_f = -24.31$ ppm/°C. And for sol–gel process, MZN powders with particle sizes of approximately 50 nm were obtained successfully. A considerable decrease in synthesis temperature (at 600 °C) was obtained in air atmosphere for the formation of MZN nanopowders with well crystallinity. Moreover, MZN ceramics with nearly full densities were obtained at 1175 °C and had excellent microwave dielectric properties of $\varepsilon_r = 22.16$, $Q{\cdot}f = 29{,}490$ GHz and $\tau_f = -15.99$ ppm/°C. Obviously, sol–gel process not only had major advantages in lowering sintering temperatures, refining microstructure, and controlling morphology and final phase composition but also improved the microwave dielectric properties of MZN ceramics.

Acknowledgments

This work was supported by the Project development plan of science and technology of ji'nan city (No.201303061), Ji'nan City Youth Science and Technology Star Project (No.2013035), and National Natural Science Foundation (No. 51472108) and Study Abroad Programs by Shandong Province Government.

References

[1] A. Terrell Vanderah, Science 298 (8) (2002) 1182–1184.
[2] R.J. Cava, J. Mater. Chem. 11 (1) (2001) 54–62.
[3] I.M. Reaney, D. Iddles, J. Am. Ceram. Soc. 89 (7) (2006) 2063–2072.
[4] D. Cruickshank, J. Eur. Ceram. Soc. 23 (14) (2003) 2721–2726.
[5] M.T. Sebastian, Dielectric Materials for Wireless Communication, Elsevier Science & Technology, 2008.
[6] W. Wang, L.Y. Li, S.M. Xiu, et al., J. Alloys Compd. 639 (5) (2015) 359–364.
[7] M. He, H.W. Zhang, J. Alloys Compd. 586 (2014) 627–632.
[8] C. Liu, H.W. Zhang, H. Su, et al., J. Alloys Compd. 646 (2015) 1139–1142.
[9] R. Muhammad, Y. Iqbal, I.M. Reaney, J. Alloys Compd. 646 (2015) 368–371.
[10] M.A. Nath, S.L. Samal, K.R. Obulesu, J. Alloys Compd. 615 (2014) 18–24.
[11] S.D. Ramarao, V.R.K. Murthy, Scr. Mater. 69 (3) (2013) 274–277.
[12] Y. Cheng, R.Z. Zuo, Y. Lv, Ceram. Int. 39 (8) (2013) 8681–8685.
[13] B.W. Hakki, P.D. Coleman, IEEE Trans. 8 (4) (1960) 402–410.
[14] W.E. Courtney, IEEE Trans. 18 (8) (1970) 476–485.
[15] E.S. Kim, C.J. Jeon, P.G. Clem, J. Am. Ceram. Soc. 95 (9) (2012) 2934–2938.
[16] B.D. Silverman, Phys. Rev. 125 (1962) 1921–1930.
[17] W.S. Kim, T.H. Kim, E.S. Kim, et al., Jpn. J. Appl. Phys. 37 (1998) 5367–5371.
[18] C.L. Huang, M.H. Weng, Mater. Res. Bull. 35 (2000) 1881–1888.
[19] H.J. Lee, K.S. Hong, S.J. Kim, et al., Jpn. J. Appl. Phys. 36 (1997) L1318–L1320.
[20] H. Tamura, J. Eur. Ceram. Soc. 26 (2006) 1775–1780.
[21] E. Schlömann, Phys. Rev. 135 (1964) A413–A419.
[22] R. Roy, Science 238 (1987) 1664–1669.